LELAND STANFORD JUNIOR UNIVERSITY
ORGANIZED 1891

STANFORD UNIVERSITY
ENGINEERING IN MEDICINE AND BIOLOGY

TRANSMISSION CHARACTERISTICS OF AXIAL WAVES IN BLOOD VESSELS

THIS WORK TO BE PRESENTED AS PAPER NO. 1350
AT THE 1968 SESA SPRING MEETING, ALBANY, N.Y.
MAY 7-10

M. ANLIKER[†]
W. E. MORITZ[‡]
E. OGDEN[‡]

[†]ASSOC. PROF., AERONAUTICS AND ASTRONAUTICS, STANFORD UNIVERSITY
[‡]PH.D. CANDIDATE AND NASA TRAINEE, DEPT. OF AERONAUTICS AND ASTONAUTICS, STANFORD UNIVERSITY
[‡]CHIEF, ENVIRONMENTAL BIOLOGY DIV., AMES RESEARCH CENTER, NASA

BIOMECHANICS LABORATORY

This work was carried out at the Ames Research Center of NASA with the support of NASA Grant NGR 05-020-223

SUDAAR NO. 343

Department of Aeronautics and Astronautics
Stanford University
Stanford, California

TRANSMISSION CHARACTERISTICS OF AXIAL WAVES IN BLOOD VESSELS

by

M. Anliker,[+] W. E. Moritz[‡]
and
E. Ogden,[‡] Ames Research Center, NASA

To be presented as
Paper No. 1350 at the 1968 SESA Spring Meeting
Albany, N.Y., May 7 - May 10

SUDAAR NO. 343
April 1968

[+] Associate Professor
[‡] Ph. D. Candidate and NASA Trainee
[‡] Chief, Environmental Biology Division

This work was carried out at the Ames Research Center of NASA
with the support of NASA Grant NGR 05-020-223

ABSTRACT

The elastic behavior of blood vessels can be quantitatively examined by measuring the propagation characteristics of waves transmitted by them. In addition, specific information regarding the viscoelastic properties of the vessel wall can be deduced by comparing the observed wave transmission data with theoretical predictions. The relevance of these deductions is directly dependent on the validity of the mathematical model for the mechanical behavior of blood vessels used in the theoretical analysis. Previous experimental investigations of waves in blood vessels have been restricted to pressure waves even though theoretical studies predict three types of waves with distinctly different transmission characteristics. These waves can be distinguished by the dominant displacement component of the vessel wall and are accordingly referred to as radial, axial and circumferential waves. The radial waves are also referred to as pressure waves since they exhibit pronounced pressure fluctuations. For a thorough evaluation of the mathematical models used in the analysis it is necessary to measure also the dispersion and attenuation of the axial and circumferential (torsion) waves.

To this end a method has been developed to determine the phase velocities and damping of sinusoidal axial waves in the carotid artery of anesthetized dogs with the aid of an electro-optical tracking system. For frequencies between 25 and 150 Hz the speed of the axial waves was between 20 and 40 m/sec and generally increased with frequency, while the natural pressure wave travelled at a speed of about 10 m/sec. On the basis of an isotropic wall model the axial wave speed should however be approximately 5 times higher than the pressure wave speed. This discrepancy can be interpreted as an indication for an anisotropic behavior of the carotid wall. The carotid artery appears to be more elastic in the axial- than in the circumferential direction.

BACKGROUND INFORMATION AND MOTIVATION

Medical researchers have long been interested in the elastic behavior of blood vessels. This interest can be attributed to a variety of ailments and, in general terms, to the vital role that the proper elastic behavior of blood vessels plays in maintaining and regulating circulation. Besides this, the question of astronauts surviving space flights involving weightlessness for months or years and high decelerations during reentry has provided an additional incentive. It is expected that the cardiovascular system of man will adapt itself so well to the weightless state that it can no longer cope with reentry conditions after a long space flight unless an exercise or conditioning program is devised for astronauts. We know from experience that after prolonged bed rest--which can be interpreted as a partial simulation of weightlessness--the cardiovascular system shows signs of deconditioning. This manifests itself by a reduced tilt-table tolerance or by orthostatic hypotension and syncope, which is attributed to an excessive diminution of the cardiac output caused by the pooling of blood in the lower parts of the body. The pooling is due either to a reduced blood volume or to a reduced ability of the veins and arteries to resist higher transmural pressures induced by the hydrostatic head.

It appears that the prolonged absence of normal stimuli such as the variation of the hydrostatic pressure with posture could cause the walls of blood vessels to become more elastic. Since gravity-induced stimuli are absent during zero-G flight, we must expect a loss of the ability of vessels to resist deformation at higher pressures, which theoretically could prove fatal during reentry conditions. To prevent this, we have to devise not only an exercise or conditioning program for astronauts, but also reliable methods of measuring changes in the elastic behavior of blood vessels. Such methods could then be used to determine the effectiveness of an exercise or conditioning program during a prolonged space flight. Besides this, they would lend themselves to various clinical applications and possibly to the early detection of atherosclerosis.

Ideally, the measurement of the distensibility and elastic properties of blood vessels should not require a penetration of the skin. A nontraumatic method could for example be based on the fact that certain characteristic features associated with the generation and transmission of sound or pulse waves in a given medium can be related to the elastic properties of that medium. It has long been known that the speed of a pressure pulse in a blood vessel is an approximate measure for the elastic behavior of that vessel. In view of the fact that the elastic behavior can change quite rapidly with time and varies with size, location and nature of the vessel, a method based on wave generation and transmission would be particularly appropriate since it yields essentially local and instantaneous values. In the case of arteries we could utilize the natural pulse wave generated by the heart as has been done for more than a century, while for veins we would have to generate an artificial pressure wave. The effective Young's modulus, E, could then be estimated with the aid of the Moens-Korteweg equation

$$V^2 = \frac{Eh}{2\rho_f a}$$

if the wave speed V, the radius of the vessel a, the wall thickness h and the blood density ρ_f are known. Estimates for E obtained in this manner from a single wave speed measurement can, however, not be expected to be sufficiently accurate to reflect reliably changes in the effective Young's modulus of the vessel wall. The Moens-Korteweg equation is based on an extremely simple mathematical model for the mechanical behavior of blood vessels and their surroundings. Moreover, with a noninvasive technique we could only measure the wave speed V and would have to use empirical values for the wall thickness to radius ratio.

A more precise quantitative description of the wave transmission characteristics in terms of the physical and geometric properties of the blood vessels is obviously needed. Also, it is necessary to measure not merely the speed of a single pressure signal but the phase velocities of various waves over a wide range of frequencies and possibly the attenuation and other characteristic features of these waves. From the speed of only one type of signal one does not obtain sufficient indication as to the validity of the mathematical model used to derive the Moens-Korteweg equation or any improvement thereof.

THEORETICAL STUDIES

Considerable effort has already been made to predict the transmission characteristics of sinusoidal pressure waves in blood vessels by utilizing various kinds of mathematical models for the mechanical behavior of arteries and veins. Significant theoretical contributions are attributed to Witzig,[1)] Iberall,[2)] Morgan and Kiely,[3)] Womersly,[4)] Hardung,[5)] Klip,[6)] and other investigators. Reviews of theoretical as well as experimental studies of waves in blood vessels and the mechanical behavior of arteries and veins in general have been made by McDonald,[7)] Fox and Saibel,[8)] Rudinger,[9)] Skalak[10)] and Fung.[11)]

From recent theoretical studies[12, 13)] we know that blood vessels can transmit three different kinds of waves if they behave like fluid-filled circular cylindrical shells. In these studies the waves are characterized by their mode shapes which are defined in terms of the displacement components u, v, w of an arbitrary point of the middle surface of the shell as illustrated in Figure 1. The waves are distinguished by the dominant displacement component at high frequencies. Accordingly we denote them as axial-, torsion- and radial-waves. Each of these three types of waves has distinctly different transmission properties. Moreover, these properties depend strongly on whether the mode shapes are axially symmetric. When we restrict ourselves to axisymmetric waves, the results of a parametric study made in references (12) and (13) reveal the following characteristic features of the three types of waves. The radial waves are only mildly dispersive and have a relatively low speed for either elastic or viscoelastic walls. They are associated with strong intraluminal pressure fluctuations and are therefore also referred to as pressure waves. The torsion waves are nondispersive for elastic vessels and mildly dispersive for viscoelastic shells. They are somewhat faster than the pressure waves and theoretically do not produce any pressure perturbations for axisymmetric modes if the fluid is inviscid. Finally, for both elastic and viscoelastic walls, the axial waves also exhibit relatively mild dispersion and have the highest speeds. When the fluid can be considered as inviscid they exhibit only minute pressure fluctuations.

The relevance of these theoretical findings depends, of course, on the validity of the mathematical model that was introduced in the analysis for the mechanical behavior of the blood vessels. Of particular significance in the prediction of the wave transmission characteristics are the constitutive laws obeyed by the vessel wall. In reference (13) the wall was assumed to be isotropically and linearly viscoelastic, incompressible and behaving like a Voigt solid in shear. Since the wall properties are unknown, they are considered as free parameters in the mathematical model and are to be determined from experimental wave transmission data. The viscoelastic properties can for example be evaluated by measuring the propagation characteristics of one type of wave. Knowing these parameters we can then predict the dispersion and attenuation of the other two types of waves and by comparing them with the transmission data obtained for such waves we can examine the overall validity of the mathematical model. By proceeding in this manner it should in particular be possible to assess the assumptions made regarding the viscoelastic and isotropic behavior of the wall.

PREVIOUS EXPERIMENTAL INVESTIGATIONS

So far, most of the experimental wave transmission studies on blood vessels have dealt with the natural pulse wave generated by the heart. Particular efforts have been made to deduce information regarding the mechanical properties of arteries from the propagation characteristics of individual harmonic components of the natural pulse.[7,14)] The results obtained in this manner are based on the assumption that arteries behave like linear systems with respect to large amplitude pressure waves. When one considers that an average pressure pulse of 40 mm Hg can produce changes in the wall stress of the order of 10% of the effective Young's modulus, the assumption of linearity must be regarded with reservation. Indeed, recent investigations[15,16)] have provided new evidence for a nonlinear behavior of the vessel wall with respect to large amplitude pressure waves.

Rather than utilizing the natural pulse wave, some investigators[17,18,19)] have artificially induced transient pressure signals by means of an injection device or an electrically driven impactor. These signals were also of large amplitude and therefore any linear analysis of them would be subject to the same criticism as that applied to the harmonic analysis of the pressure wave generated by the heart.

The propagation characteristics of waves in a given medium are usually described by the dispersion and attenuation of <u>small</u> harmonic signals, i.e. by the speed and decay of infinitely long sinusoidal waves as a function of frequency or wave length. Since we have in reality signals of finite length and media of finite dimensions that may exhibit nonlinear phenomena, the determination of these properties can in some cases be encumbered by uncertainties and may generally require laborious computations. The uncertainties arise when the waves are not sufficiently small or conditions prevail that do not justify the assumption of a linear behavior of the system or when reflections modify the transient signals of interest. Extensive computations may have to be performed when the wave is of arbitrary shape since then the Fourier transform of the propagating signal has to be evaluated at various locations within the medium if its wave transmission characteristics are to be described in terms of the speed and attenuation of harmonic waves as a function of frequency.

For a mildly dispersive medium, i.e. one in which the phase velocity varies no more than a few per cent whenever the frequency is changed by, say 10 per cent, the need for Fourier transform computations can be circumvented if the transient signal is of the form of a finite train of sine waves. As shown in Figure 2, the Fourier spectrum of such waves is dominated by the frequency of the sine waves in increasing propertion to the length of the trains. Therefore, the speed of such a signal can be considered a good approximation of the phase velocity corresponding to the frequency of the sine waves. Also, it is possible to avoid the interference of reflections with the transient signal if the signals are of sufficiently short duration or if the medium exhibits strong attenuation. For sufficiently high frequencies and short trains the waves can be recorded before their reflections arrive at the recording site. In the case of strong attenuation, the reflections of a small wave may be completely damped out before they reach the transducer location.

This approach has been successfully applied in a recent investigation of the dispersion and attenuation of pressure waves (radial waves) in the thoracic aorta of anesthetized dogs.[16] The results of this study show that for frequencies between 40 and 200 Hz the aorta exhibits only mild dispersion but exhibits strong attenuation that can largely be attributed to dissipative mechanisms in the vessel wall. At normal blood pressure levels the wave speed during diastole can have a value between 4 and 6 m/sec. Moreover, for all frequencies considered, the amplitude ratio of propagating waves exhibits the same exponential decay pattern with distance measured in wavelengths.

While these results allow for the partial validation of a mathematical model for the mechanical behavior of blood vessels, a thorough evaluation of the model requires also a study of the transmission characteristics of axial- and torsion-waves. To this end we have extended the method used for pressure waves to measure also the dispersion and attenuation of axial waves. In view of the lack of accessibility of the thoracic aorta for the generation of axial waves the carotid artery was selected for the experimental investigation described in this report.

DESCRIPTION OF EXPERIMENTS

The authors have induced finite trains of sinusoidal axial displacements in the walls of surgically exposed carotid arteries of anesthetized dogs. The animals were mature male mongrels of unknown age. They weighed between 20 and 40 kg and were anesthetized with approximately 30 mg/kg sodium pentobarbital (Nembutal). Throughout the experiments the dogs were kept in the supine position.

The surgical procedure consisted of a midline incision approximately 20 cm long on the ventral side of the neck and separating segments of the right and left carotid arteries from the surrounding tissue. Care was taken to minimize the surgical trauma and dehydration of the vessels in an effort to avoid excessive changes in the physiological conditions. As shown in Figure 3, the common carotid arteries in the dog originate from the brachiocephalic artery and supply blood to the neck and head. Since the first branch of the carotid (cranial thyroid) is located about 15 to 20 cm above the brachiocephalic we thus have an unusually long section of a branch-free vessel of nearly constant geometry. To allow for a comparison of the wave transmission data with theoretical predictions, the wall thickness and radius of the carotid artery were measured in 12 dogs and the initial axial stretch was determined in 5 animals. These measurements were made with the aid of a caliper and the data are given in Table I.

After exposure of the vessels the speed of the natural pulse wave in the right carotid was determined by inserting the needles from pressure transducers (see Figure 4) into the lumen at two different points 3.5 to 8 cm apart and by recording the local pressure as a function of time. The distances between the needle tips were determined to an accuracy of .1 cm by making use of an X-ray fluoroscope equipped with an image intensifier and of a radio-opaque grid with a mesh size of 1 cm. As pressure transducers we used commercially available Bytrex pressure cells model HFD-5 that were imbedded in modified standard 3-way stopcocks. This arrangement provided for easy attachment of various size needles and for flushing the chamber and needle during the course of the experiment. The Bytrex pressure cell has a fundamental frequency of 60 kHz in air and is linear within 1% from 0 to 300 mm Hg.

The output from the bridge circuit was amplified by means of an Astrodata Model 885 DC amplifier and the signals were then recorded by a Honeywell Visicorder with galvanometers whose frequency response is flat up to 3300 Hz. A tracing of a representative pressure recording obtained at a paper speed of 25 cm/sec is shown in Figure 5.

The needles from the Bytrex pressure sensing device were then removed from the carotid and a rigid catheter attached to a Statham P23Dd manometer was placed into the vessel. To provide an indication of the arterial pressure at the root of the left carotid the catheter was advanced into the brachiocephalic artery. The blood pressure was monitored during the entire experiment as an indicator of the general physiological condition of the animal.

Small target collars weighing less than .5 gm (Figure 6) were attached to the left carotid 4 to 11 cm apart. They consisted of 4 mm sections of plastic tubing provided with a slit and silk threads to secure the target to the vessel. To limit the constriction of the vessel to less than 15% of its diameter various collars of different internal diameters were available. Paper targets as shown in Figure 6 with a line of contrast in reflectivity were then glued into place on each of the collars.

The motion of the targets was monitored with the aid of a pair of PhysiTech*) Model 39A electro-optical tracking units with lens configurations allowing for a resolution of 2×10^{-4} cm and a frequency response in excess of 2000 Hz. Target illumination was provided by a quartz iodine light powered by a DC source. The outputs from the tracking units were recorded on the Honeywell system described above with a paper speed up to 2m/sec.

In some experiments, the axial wall motion associated with the natural cardiac cycle was monitored. A tracing of a representative recording is shown in Figure 7.

To generate transient axial waves the plastic collar device shown in Figures 8 and 9 was then attached to the vessel 3 to 5 cm distal from the first target. Again, various sizes were available to adapt to the individual artery.

*) PhysiTech, Inc.
645 Davisville Road
Willow Grove, Pa. 19090

The collar-artery interface was padded with short pieces of braided umbilical tape to insure good mechanical coupling. In all cases the constriction of the vessel radius was less than 15% .

The electromagnetic shaker is shown in Figure 10. It consists of a solenoid whose core is connected to a lightweight piston. The device is driven by an electronic oscillator and a high fidelity amplifier which is gated by a tone burst generator. When the shaker was activated, axial wall displacements in the form of finite trains of sine waves were generated. The frequency and amplitude of these displacements were controlled by the electronic oscillator while the number of sine waves contained in the trains and the intervals between successive trains were determined by the tone burst generator. In the experiments described here the frequency range was 25 to 150 Hz and the amplitude was usually less than 2 mm peak-to-peak and in no case more than 3.5 mm. In attaching the plastic collar to the piston the natural stretch of the vessel was kept unchanged. Moreover the piston axis was carefully aligned with the axis of the carotid to minimize the possibility of generating non-axisymmetric waves in the vessel.

Theoretical considerations[12, 13)] predict that non-axisymmetric waves of all three types (radial-, torsion- and axial- waves) have vastly different propagation characteristics than do their corresponding axisymmetric waves. In contrast to the axisymmetric waves, they exhibit strong dispersion and an attenuation per wave length that varies strikingly with frequency and therefore they would readily be recognized among axisymmetric signals. However, no evidence of their presence would be discerned from our recordings.

Figure 11 shows the targets, collar and shaker in place. The view seen by the optical trackers is shown in Figure 12. A sample tracing of a typical Visicorder record is shown in Figure 13.

Both the Statham transducer and the optical tracking units including all amplifiers and recording instruments were calibrated as a system for each experiment.

In some experiments the pressure fluctuations within the vessel at the target locations were monitored together with the axial wall displacements. This was accomplished with the aid of highly sensitive capacitance pressure transducers originally designed for wind tunnel model studies and adapted for physiological applications. The transducers used had a diameter of 1.5 mm and were mounted on a flexible catheter that encloses the electrical leads and a venting tube (see Figure 14). The cells form part of a capacitance bridge and signals are recorded after amplification by a 100 kHz carrier amplifier. Their fundamental frequency is 82 kHz in air, and they have a resolution of about .2 mm Hg and are linear within 1% from 0 to 200 mm Hg.

The catheter-tip manometers were inserted either through the cranial thyroid artery or one of the femoral arteries. In the latter case it was necessary to manually guide the transducers from the brachiocephalic into the carotid artery. To this end the chest was opened and the animal artificially ventilated with room air at the rate of 8 to 10 liters per minute by means of a Palmer respirator. The transducers were positioned at the same cross-section as the external targets with the X-ray fluoroscope.

The axial motion of the collar generated pressure waves as well as axial waves. It appears that the pressure waves were induced by the axial displacement of the constricted cross-section at the site of the vibrating collar. A tracing of a representative recording of both types of waves is given in Figure 15.

DATA REDUCTION

The speed of the natural pulse wave was determined in the usual manner by measuring the time of propagation of the wave front (Δt) over the distance (Δx) between the points at which the pressure was monitored. There are various ways in which the time of propagation of the front of the natural pulse wave can be defined and the resulting Δt may depend on the choice. For example, we may define it as the time of propagation of a characteristic point of the wave front, say the point corresponding to 1/3 of the pulse pressure, or we can choose, as shown in Figure 5, the intersection of the tangent in the inflection point of the wave front with a line approximating the terminal phase of the preceding pulse. In this study we consistently made use of the latter definition.

By contrast, the speed of the artificially induced trains of sine waves could be determined with far greater certainty. The mildly dispersive nature of the carotid artery with respect to small axisymmetric radial and axial waves and the absence of reflection interference made it possible to measure the speed of such signals virtually independently of the selection of a characteristic point. As illustrated in Figure 13, we have chosen as characteristic points the intersection of the tangents to the sine waves in two successive inflection points. At a recording speed of 100 cm/sec or higher the time difference Δt could be determined to an accuracy of .3 milliseconds. With Δt ranging from 2.5 to 10 milliseconds depending on the nature of the wave and on the distance Δx between the observation points, the relative error for Δt was between 3 and 12%. Considering in addition that the absolute error of Δx was $\pm .1$ cm and that Δx usually had a value of about 10 cm, the largest possible relative error for a single speed measurement was between 4 and 13%.

Guided by the observations in reference (16) regarding the attenuation of small sinusoidal pressure waves in the aorta, we evaluated the ratio of the amplitudes of the axial waves as a function of the propagation distance Δx measured in wave lengths. The amplitude is defined as illustrated in Figure 13 and since A diminishes in an exponential fashion with distance, the ratio A/A_0 is plotted on a logarithmic scale versus $\Delta x/\lambda$ (λ = wavelength).

RESULTS AND DISCUSSION

At normal blood pressure levels the speed of the natural pulse wave in the exposed carotid artery of 4 dogs was found to have a value between 8.5 and 12.4 m/sec with an average of 10.2 m/sec. The wave speed was determined from pressure recordings such as those shown in Figure 5. Theoretically it should be possible to evaluate the speed also from the recordings of the axial displacements induced by the natural pulse. However, as is evident from Figure 7, the axial wall motion due to the natural pulse is extremely small and highly damped even when the carotid is fully exposed. Moreover, it appears that the motion of the heart during the cardiac cycle also contributes to the axial wall motion of the carotid.

From the recordings of the artificially induced axial waves it can be seen that the finite trains of sine waves retain their sinusoidal character during propagation for all frequencies. This may be interpreted as an indication that the carotid artery can not be strongly dispersive with respect to axisymmetric axial waves in the frequency range considered. Further substantiation of this conclusion is the independence of the transmission time Δt with respect to the selection of a characteristic point. Finally the plots of signal speed versus frequency as shown in Figures 16 and 17 corroborate the weak frequency dependence of the signal speed. They may therefore be interpreted as a good approximation of the corresponding phase velocity. As expected on the basis of theoretical studies,[20, 21, 22)] the phase velocity of the axial waves increases with frequency.

At the target closest to the vibration collar the amplitude of the axial displacement was always less than 2.5 mm. A variation of the amplitude up to this limit did not have a noticeable effect on the signal speed. Likewise, the naturally occurring fluctuations in pressure and flow did not cause any obvious effects on the speed of the axial waves. The absence of an amplitude effect on the speed of the axial waves suggests that the carotid artery behaves like a linear system with respect to such waves.

The attenuation data given in Figures 18 and 19 have been obtained by measuring the amplitudes of the axial waves at two fixed stations as a function of frequency. It appears that the amplitude ratio portrays a similar exponential and frequency-independent decay pattern with distance in wavelengths as do the pressure waves in the aorta.[16]

$$\frac{A}{A_o} = e^{-k\frac{\Delta x}{\lambda}}$$

However, the attenuation coefficient k for axial waves in the exposed carotid ranges from 2.8 to 7.2, while for pressure waves in the aorta it was found to be between .7 and 1.0. The rapid decay of the amplitude of axial waves can be attributed to the viscosity of the blood and to strong dissipative mechanisms in the vessel wall. The radiation of energy into the surrounding medium can be disregarded since the carotid was fully exposed.

On three dogs the axial wall motion and the intraluminal pressure fluctuations on the carotid were monitored simultaneously. The results show (see Figure 15) that the speed of the axial waves is approximately 3 times higher than that of the pressure waves. However, according to theoretical predictions[12,13] the axial wave speed should be approximately 5 times greater than the speed of the radial waves if the vessel wall is isotropically elastic or viscoelastic. This discrepancy can therefore be interpreted as an indication of an anisotropic behavior of the exposed carotid artery. Specifically, it implies that under in-vivo conditions the exposed carotid is more elastic in the axial- than in the circumferential direction. In this regard our results confirm the observations made by Fenn[23] on various excised dog arteries including the carotid.

CONCLUSIONS

At normal blood pressure levels the surgically exposed carotid artery of anesthetized dogs exhibits mild dispersion and strong attenuation with respect to artificially induced axial waves with frequencies between 25 and 150 Hz. The attenuation can be attributed to the viscosity of the blood and to dissipative mechanisms in the carotid wall. The carotid artery appears to behave like a linear system with respect to small axial waves over a relatively wide range of transmural pressures. In addition there is evidence indicating an anisotropic wall behavior. Specifically, the carotid seems to be more elastic in the axial- than in the circumferential direction.

ACKNOWLEDGMENT

This work was carried out at the Ames Research Center of the National Aeronautics and Space Administration with the support of Grant NGR 05-020-223.

REFERENCES

1. Witzig, K., Über erzwungene Wellenbewegungen zäher, inkompressibler Flüssigkeiten in elastischen Röhren. Inaugural Dissertation, Universität Bern, Wyss 1914.

2. Iberall, A.S., Attenuation of Oscillatory Pressures in Instrument Lines, Journal of Research, National Bureau of Standards. Research Paper RP2115, Vol. 45, July 1950, pp. 85-108.

3. Morgan, G.W. and Kiely, J.P., Wave Propagation in a Viscous Liquid Contained in a Flexible Tube, J. Acoust. Soc. Am., Vol. 26, No. 3, May 1954, pp. 323-328.

4. Womersley, J.R., An Elastic Tube Theory of Pulse Transmission and Oscillatory Flow in Mammalian Arteries, WADC Technical Report TR 56-614, Wright Air Development Center, Ohio, Jan. 1957.

5. Hardung, V., Propagation of Pulse Waves in Viscoelastic Tubings, Handbook of Physiology, Circulation, Vol. 1, American Physiological Society, 1962, pp. 107-135.

6. Klip, Willem, Velocity and Damping of the Pulse Wave, Martinus Nijhoff, The Hague, 1962.

7. McDonald, D.A., Blood Flow in Arteries, Edward Arnold Ltd., London, 1960.

8. Fox, E.A. and Saibel, Edward, Attempts in the Mathematical Analysis of Blood Flow, Trans. Soc. Rheol. VII, 1963, pp. 25-31.

9. Rudinger, G., Review of Current Mathematical Methods for the Analysis of Blood Flow, Biomedical Fluid Mechanics Symposium, 1966, ASME, New York, pp. 1-33.

10. Skalak, R., Wave Propagation in Blood Flow, Biomechanics, App. Mech. Division, ASME, Ed. Y.C. Fung, 1966, pp. 20-40.

11. Fung, Y.C., Biomechanics, its Scope, History and Some Problems of Continuum Mechanics in Physiology, J. App. Mech. Reviews, Vol. 21, No. 1, Jan. 1968, pp. 1-20.

12. Anliker, M. and Maxwell, J.A., The Dispersion of Waves in Blood Vessels, Biomechanics Symposium, ASME, New York, 1967, pp. 47-67.

13. Maxwell, J.A. and Anliker, M., The Dissipation and Dispersion of Small Waves in Arteries and Veins with Viscoelastic Wall Properties, accepted for publication in Biophysical Journal.

14. Attinger, E.O., Ed., Pulsatile Blood Flow: Proceedings, Blakiston Division, McGraw-Hill Book Co., New York, 1964.

15. Dick, D., Kendrich, J., Matson, G. and Rideout, V.C., Measurement of Nonlinearity in the Arterial System of the Dog by a New Method, Cir. Res. 22, Feb. 1968, pp. 101-111.

16. Anliker, M., Histand, M.B. and Ogden, E., Dispersion and Attenuation of Small Artificial Pressure Waves in the Aorta, SUDAAR Report No. 342, Department of Aeronautics and Astronautics, Stanford University, Stanford, California, 1968.

17. Landowne, Milton, A Method Using Induced Waves to Study Pressure Propagation in Human Arteries, Cir. Res., Vol. V, Nov. 1957, pp. 594-601.

18. Landowne, Milton, Characteristics of Impact and Pulse Wave Propagation in Brachial and Radial Arteries, J. Appl. Physiol. 12(I), 1958, pp. 91-97.

19. Peterson, Lysle H., The Dynamics of Pulsatile Blood Flow, Cir. Res., Vol. II, March 1954, pp. 127-139.

20. Atabek, H.B. and Lew, H.S., Wave Propagation through a Viscous Incompressible Fluid Contained in an Initially Stressed Elastic Tube, Biophysical Journal, Vol. 6, 1966, pp. 481-503.

21. Klip, W., Van Loon, P. and Klip, D., Formulas for Phase Velocity and Damping of Longitudinal Waves in Thick-Walled Viscoelastic Tubes, J. App. Physics, Vol. 38, No. 9, August 1967, pp. 3745-3755.

22. Jones, E., Chang, I-Dee and Anliker, M., Effects of Viscosity and External Constraints on Wave Transmission in Blood Vessels, SUDAAR Report No. 344, Department of Aeronautics and Astronautics, Stanford University, Stanford, California, 1968.

23. Fenn, W.O., Changes in Length of Blood Vessels on Inflation, Tissue Elasticity, Ed. J.W. Remington, Am. Physiological Soc., 1957, pp. 154-160.

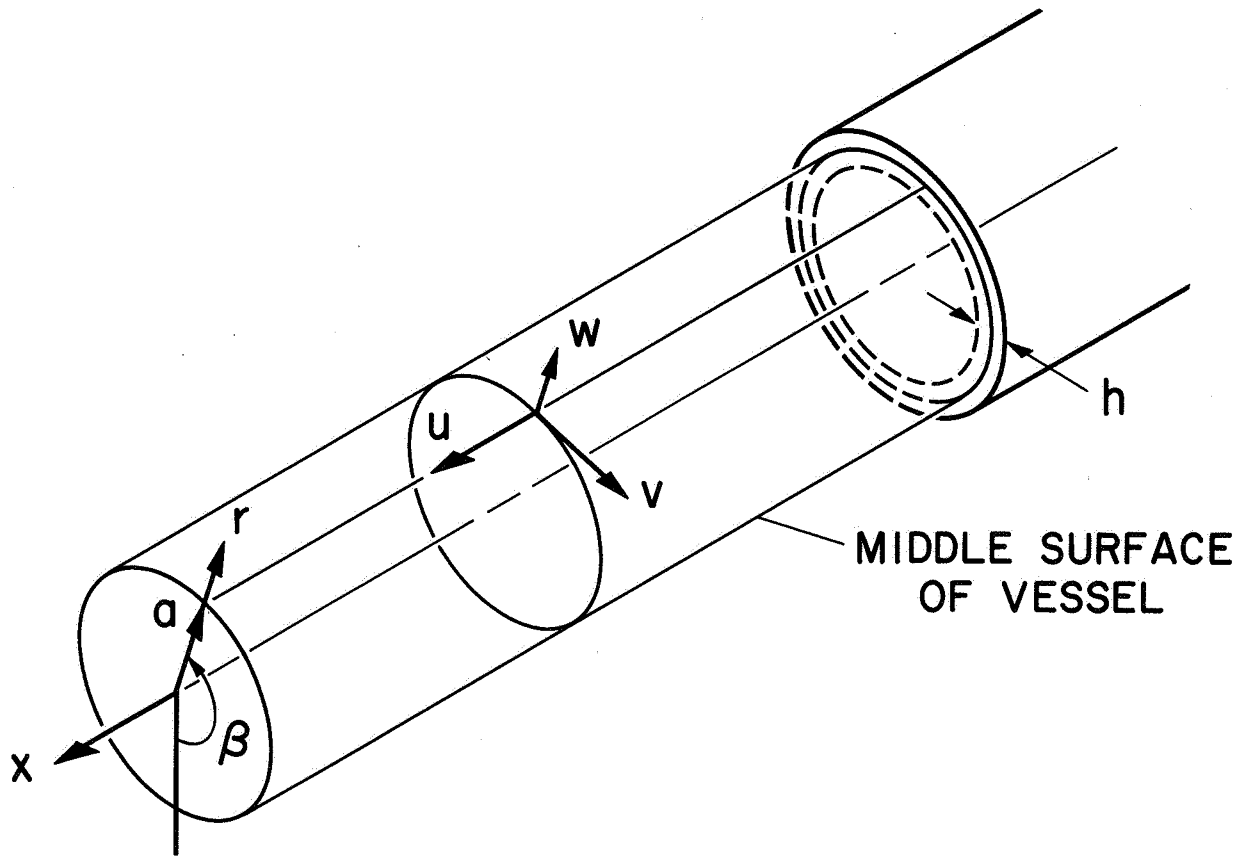

Figure 1. Coordinate system and displacement components u, v, w of an arbitrary point of the middle surface of circular cylindrical shell model for arteries.

$$f(t) = \frac{1}{2\pi} \int_{-\infty}^{\infty} F(\omega)\, e^{i\omega t}\, d\omega \qquad F(\omega) = \int_{-\infty}^{\infty} f(t)\, e^{-i\omega t}\, dt$$

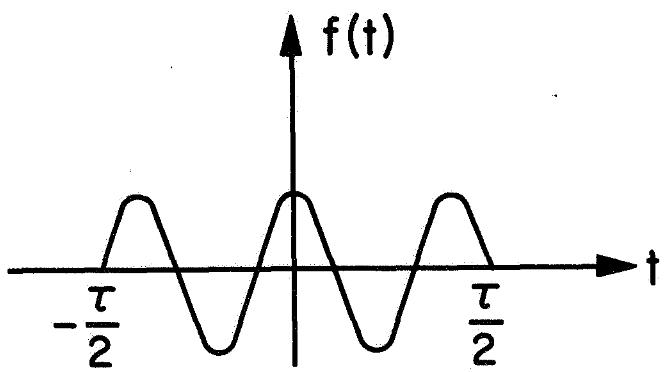

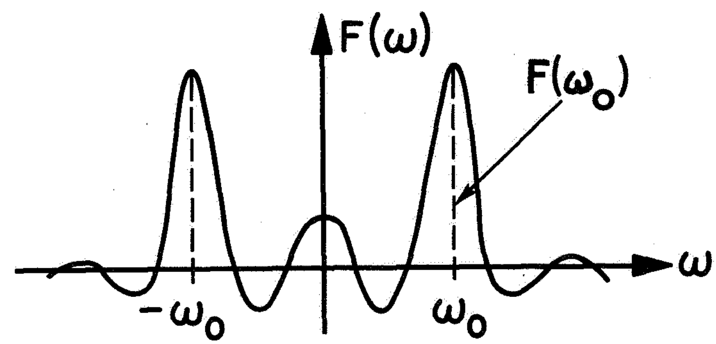

$$f(t) = \begin{cases} \cos(\omega_0 t), & |t| < \frac{\tau}{2} \\ 0, & |t| > \frac{\tau}{2} \end{cases}$$

$$F(\omega) = \frac{\tau}{2} \left[\frac{\sin\left(\frac{\omega - \omega_0}{2}\right)\tau}{\left(\frac{\omega - \omega_0}{2}\right)\tau} + \frac{\sin\left(\frac{\omega + \omega_0}{2}\right)\tau}{\left(\frac{\omega + \omega_0}{2}\right)\tau} \right]$$

Figure 2. Fourier transform of finite train of sine waves. $F(\omega_0)$ dominates the spectrum increasingly with the length of the train.

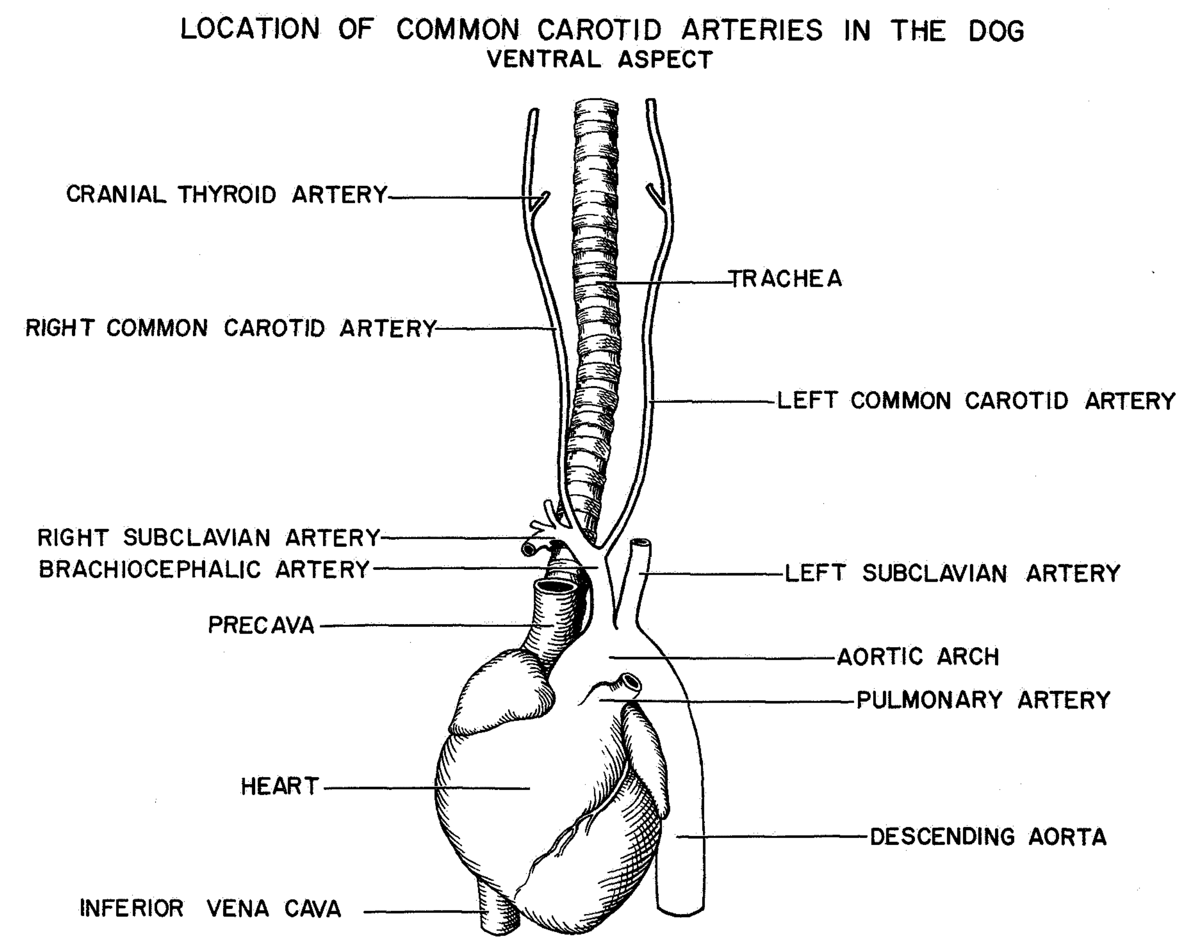

Figure 3. Pertinent anatomy of the neck region of the dog showing the location of the carotid artery with respect to the trachea and heart.

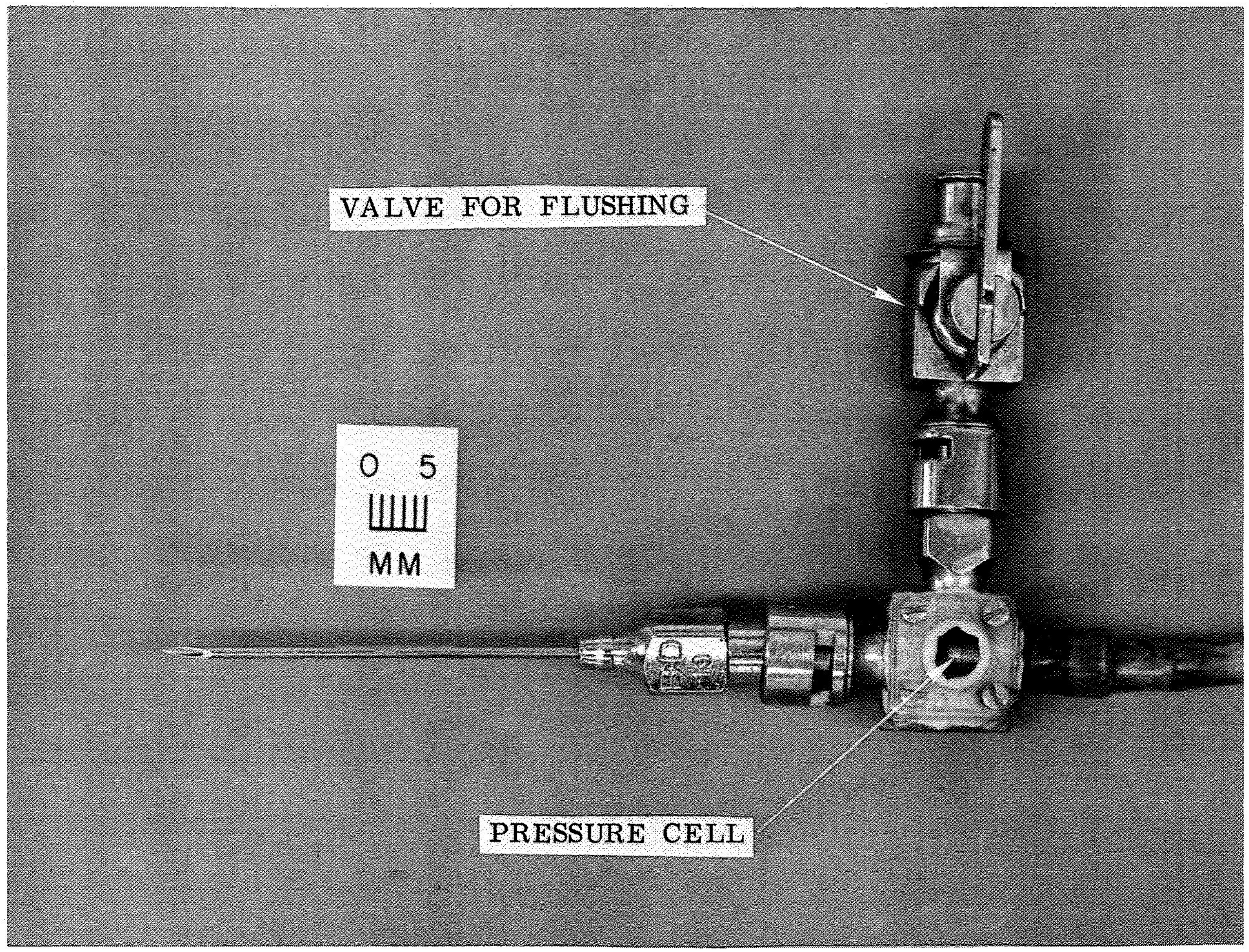

Figure 4. Pressure transducer consisting of Bytrex pressure cells HFD-5 built into a modified 3-way stopcock with needle attached.

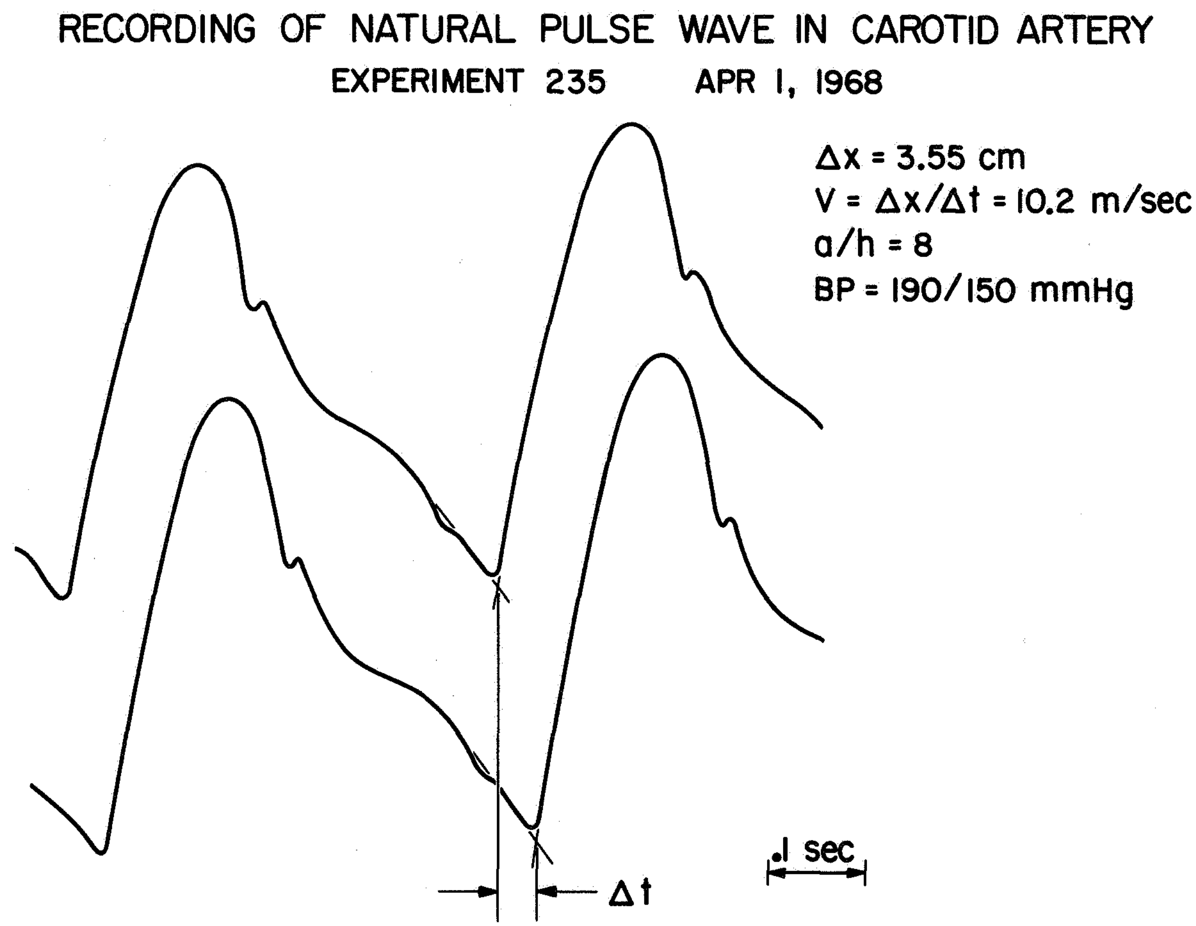

Figure 5. Representative tracing of natural pulse wave in right carotid. The pressure records were obtained with the aid of two pressure transducers of the kind shown in Figure 4. Δx denotes the distance between the needle-tips and Δt the corresponding transmission time. V = signal velocity, $\frac{a}{h}$ = radius to wall-thickness ratio and BP = blood pressure.

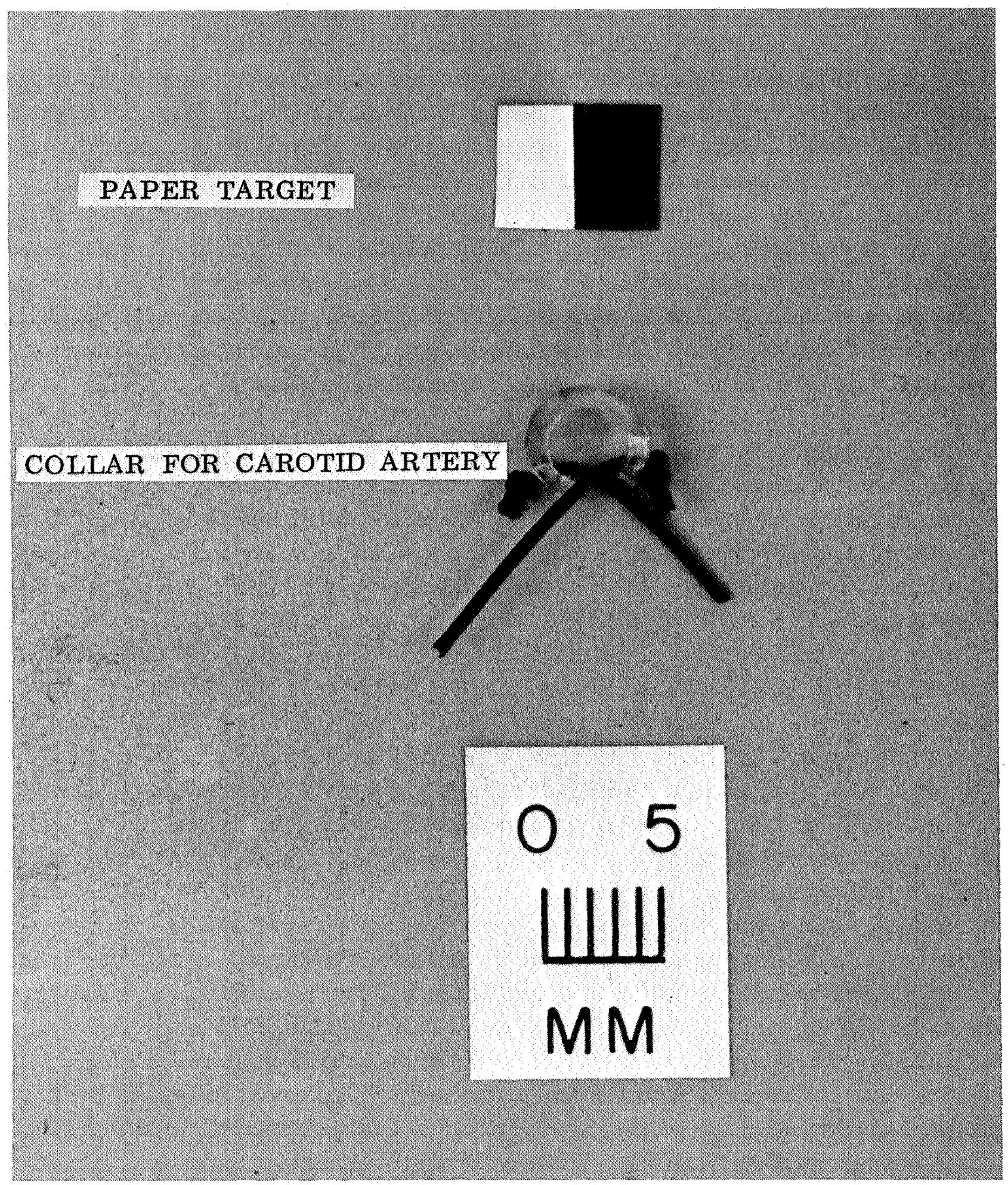

Figure 6. Plastic collar with a width of 4 mm and threads to secure it to the vessel. Paper target shown was glued on the collar. Weight of target and collar is less than .5 gm.

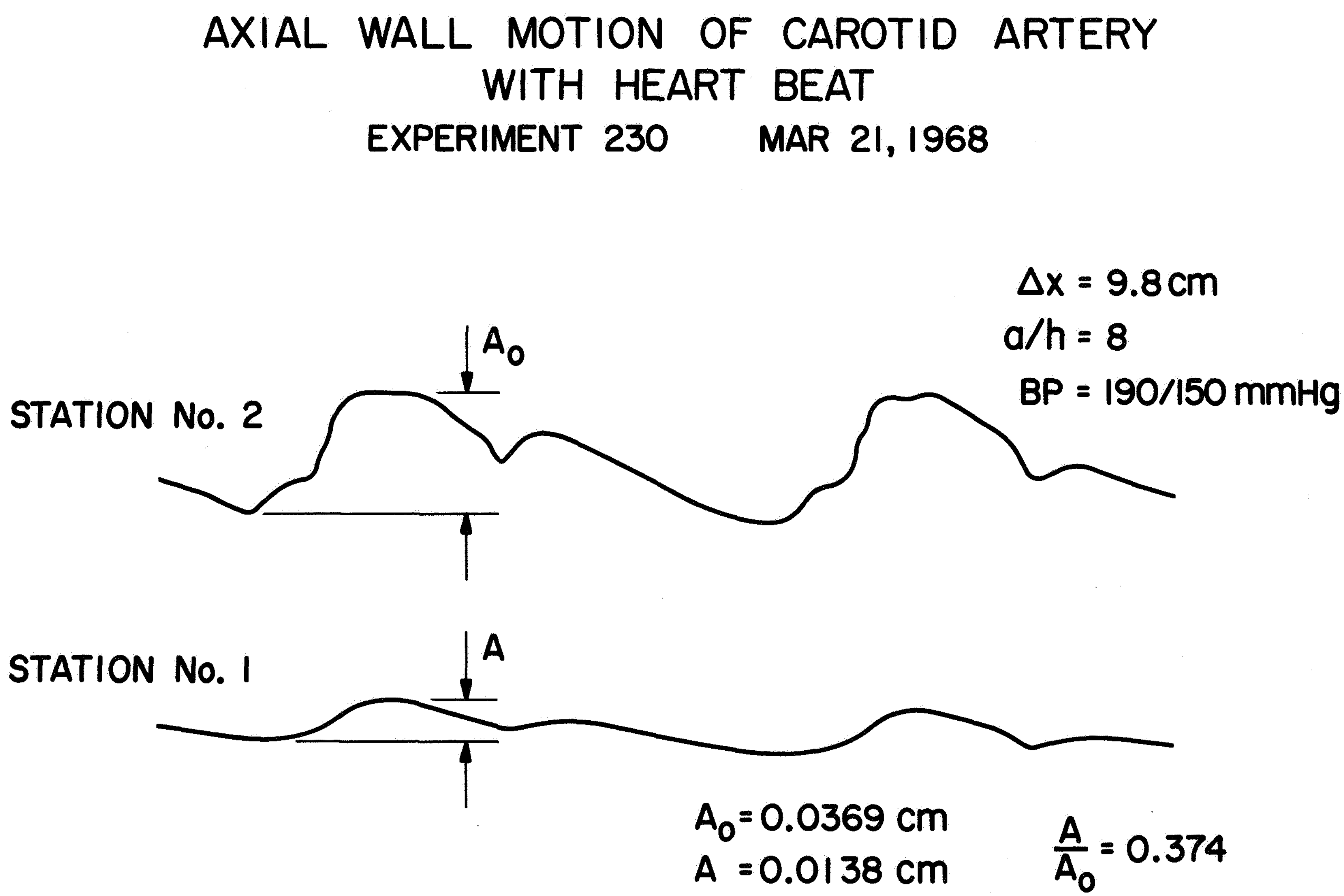

Figure 7. Tracing of axial wall motion of exposed carotid artery with heart beat. The motion was recorded with the aid of an electro-optical tracking system. Station 2 is nearer to the heart. Note strong attenuation.

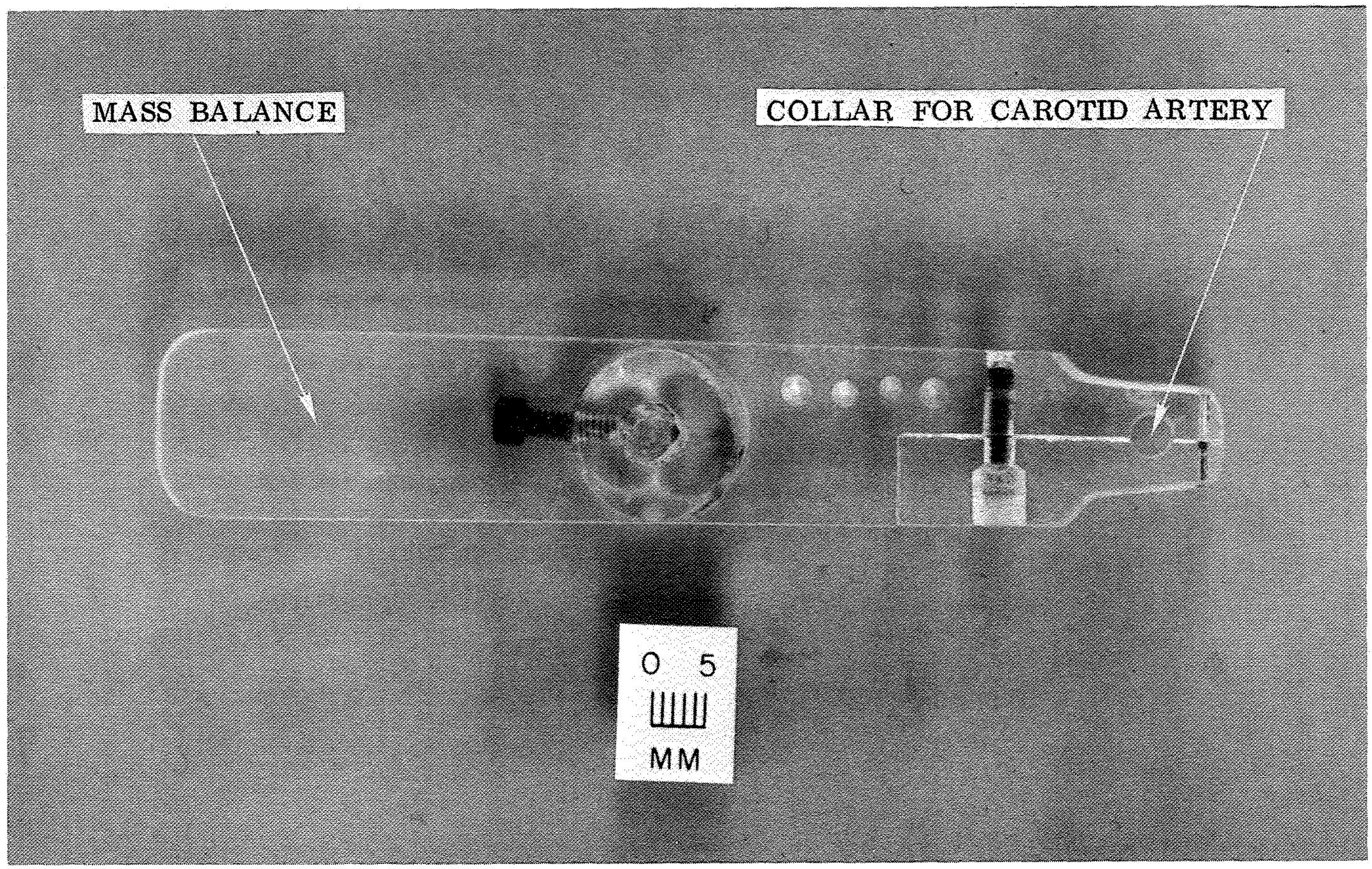

Figure 8. Front view of assembled vibrating collar device made of plexiglass.

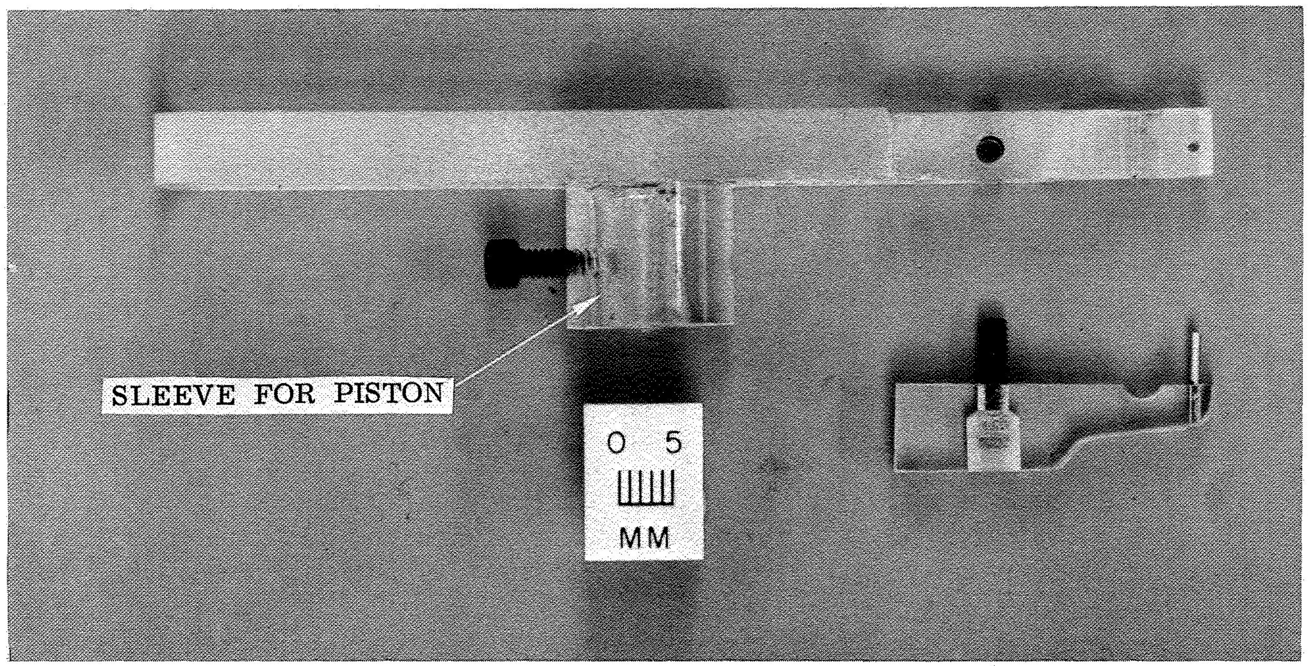

Figure 9. Side view of dis-assembled vibrating collar device.

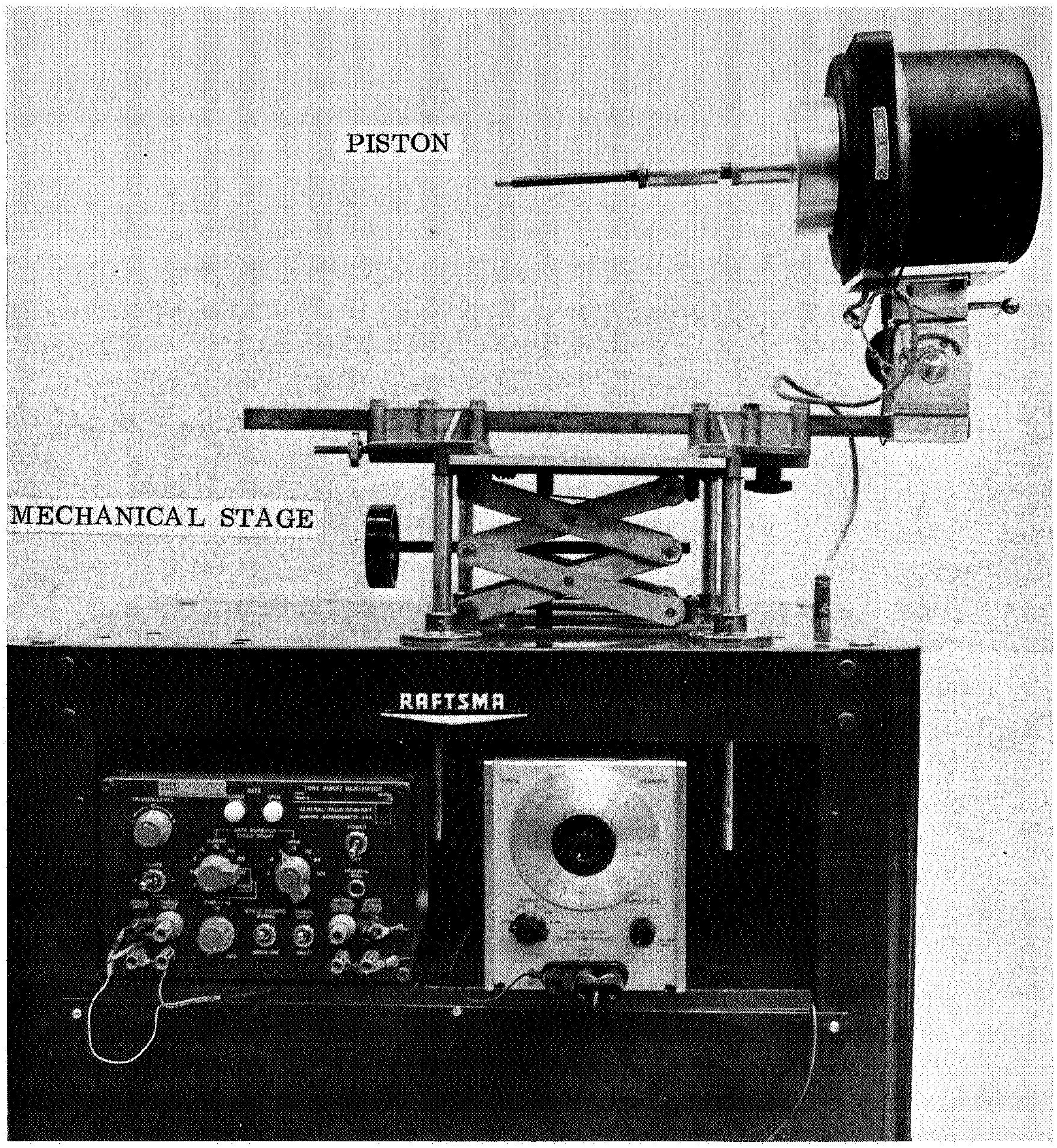

Figure 10. Electromagnetic shaker with electronic oscillator and tone burst generator. To generate axial wall motion the end of the piston is attached to vibrating collar device shown in Figures 8 and 9.

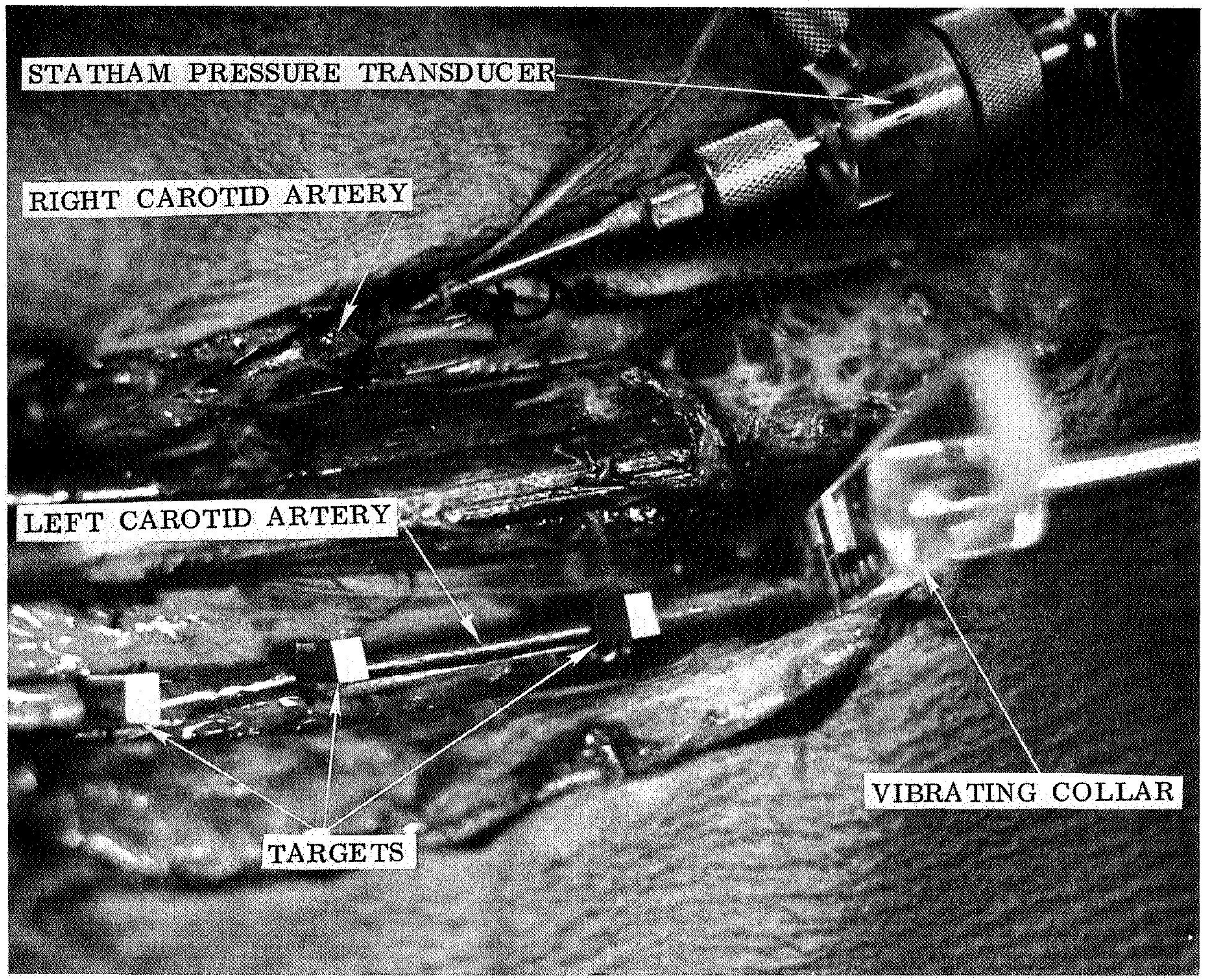

Figure 11. Surgically exposed carotid arteries. Targets and vibrating collar attached to left carotid, cannula from Statham transducer inserted into right carotid. In this instance three targets were attached to the left carotid.

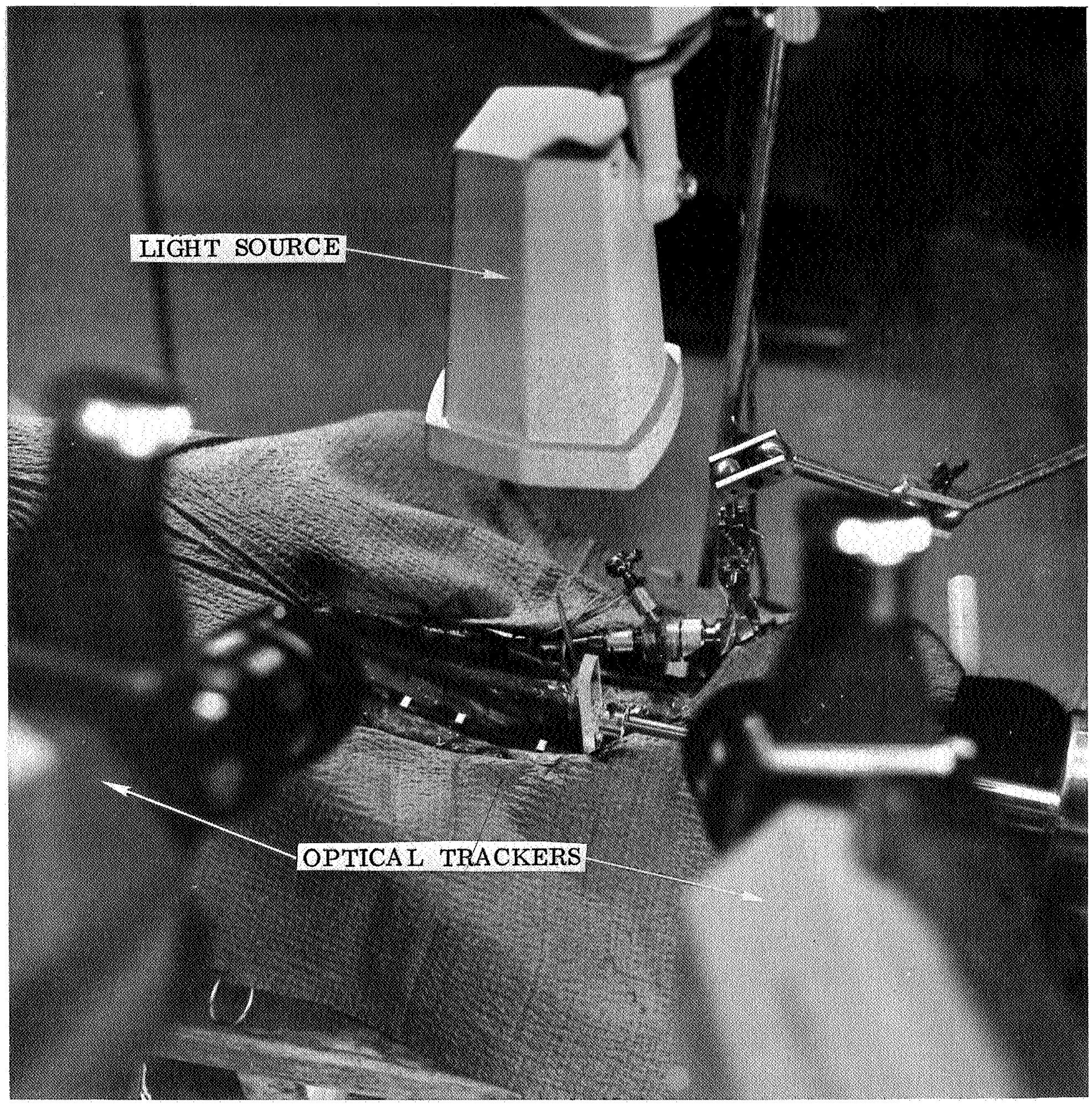

Figure 12. View of experimental arrangement with PhysiTech electro-optical trackers. Distance between lenses and targets was approximately 33 cm.

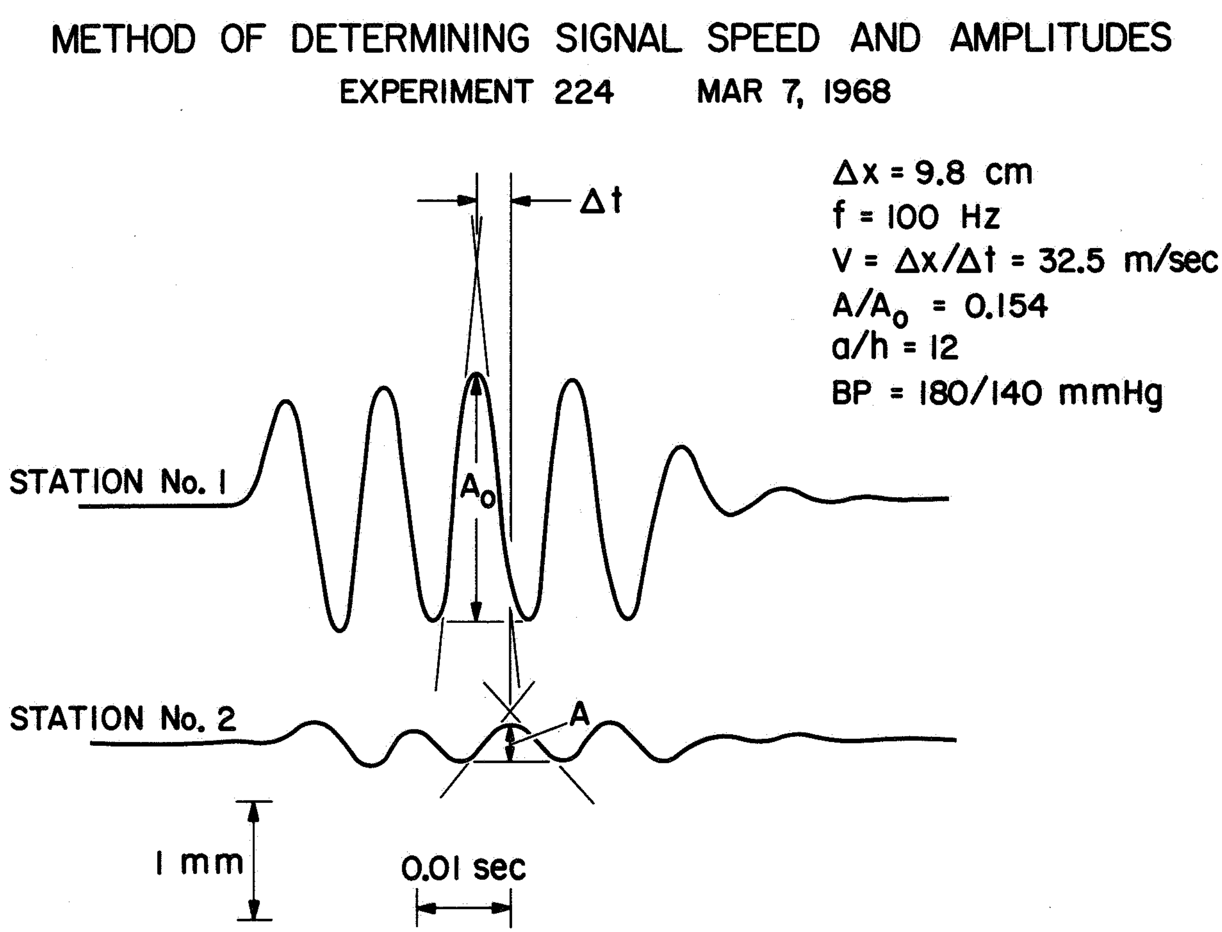

Figure 13. Tracing of artificially induced axial wall displacements in the form of a finite train of sine waves with a frequency of 100 Hz. As indicated, the signal speed is defined by the target separation Δx and the transmission time Δt of the intersection of the tangents in two successive inflection points of the sinusoidal wave train. The peak-to-peak amplitudes of the sine waves are determined as shown. Note that the sine waves are highly damped but retain their sinusoidal character during propagation.

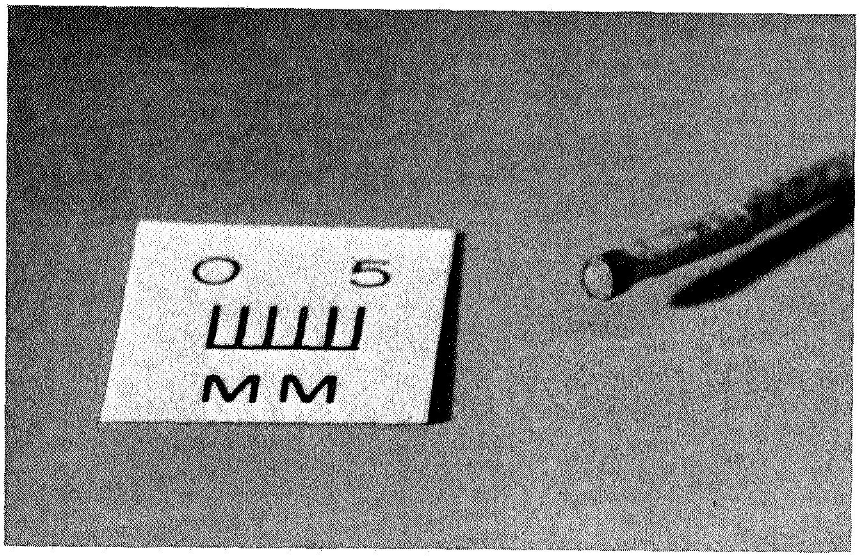

Figure 14. Capacitance-type pressure transducer mounted on a flexible catheter for physiological applications. Diameter = 1.5 mm. Resolution ≈ .2 mm Hg.

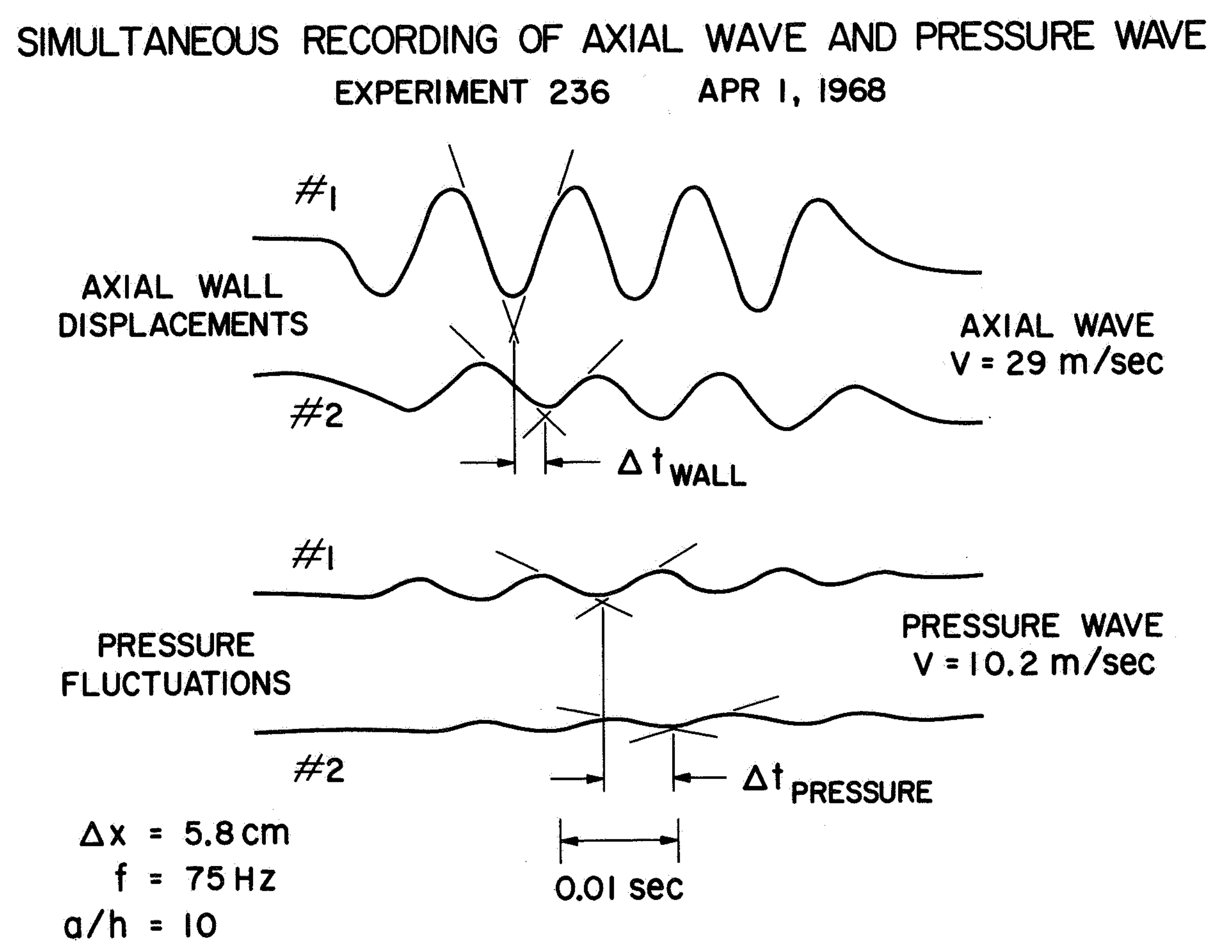

Figure 15. Tracings of simultaneous recordings of pressure- and axial waves in the left exposed carotid artery. Both types of waves were induced simultaneously by the vibrating collar. The pressure recordings were obtained with the aid of catheter-tip manometers of the kind shown in Figure 14. The manometers were located at the same cross-sections as the external targets by means of a fluoroscope. In this instance, the blood pressure was 205/170 mm Hg. Note the difference in transmission time for the two types of waves.

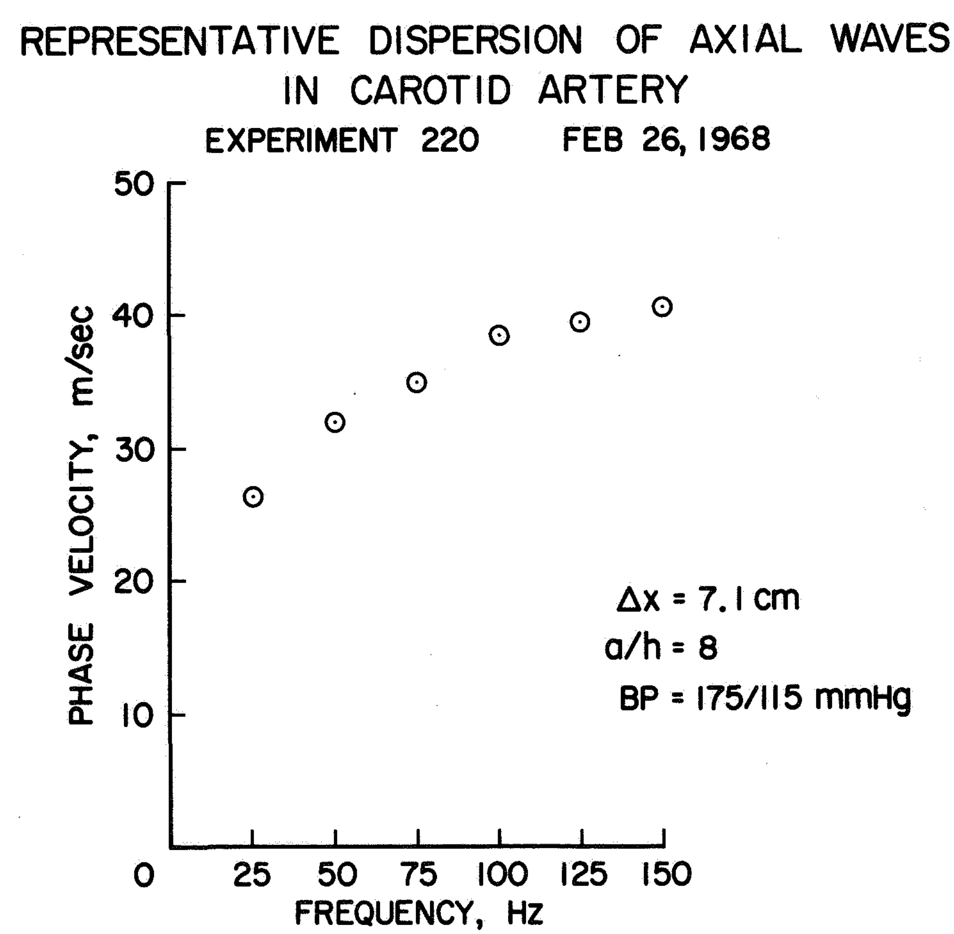

Figure 16. Typical plot of axial wave speed versus frequency in the exposed left carotid. Each point corresponds to an average of at least 5 separate wave speed measurements from recordings taken over a period of less than 5 seconds.

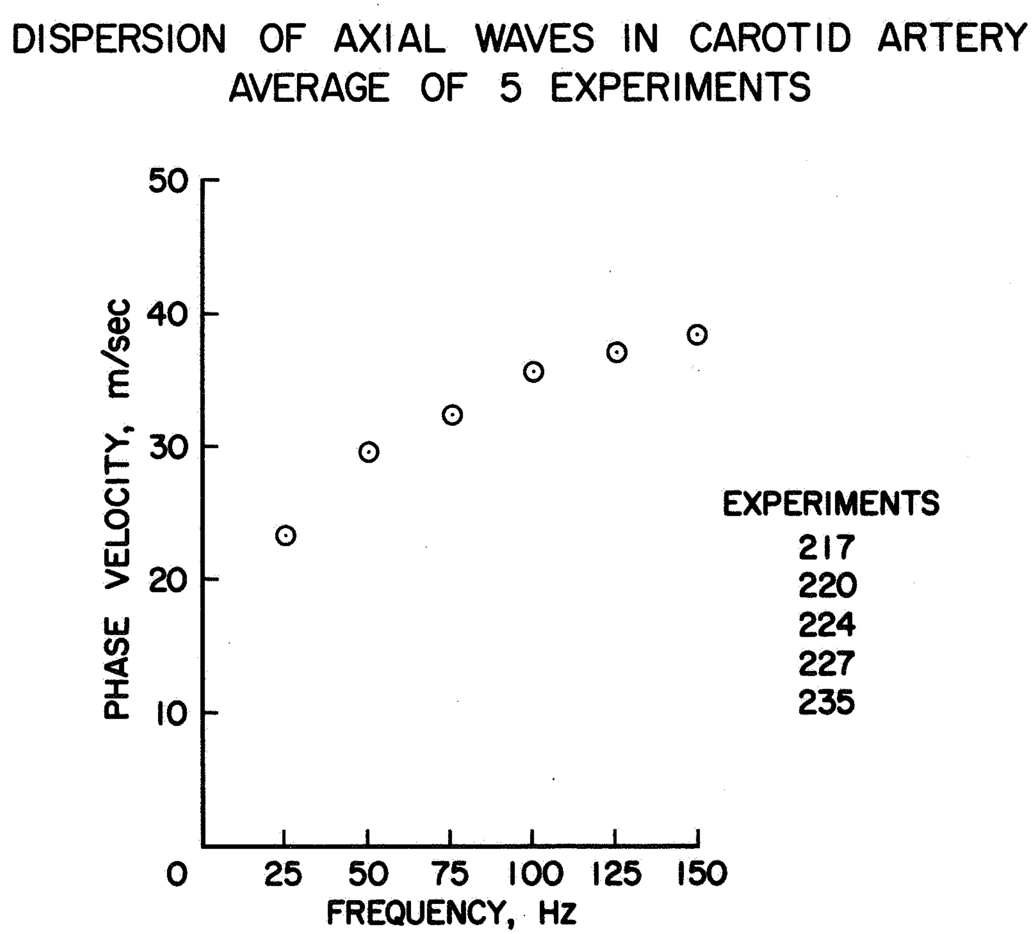

Figure 17. Average of axial wave speed measurements made on the exposed carotid arteries of 5 dogs.

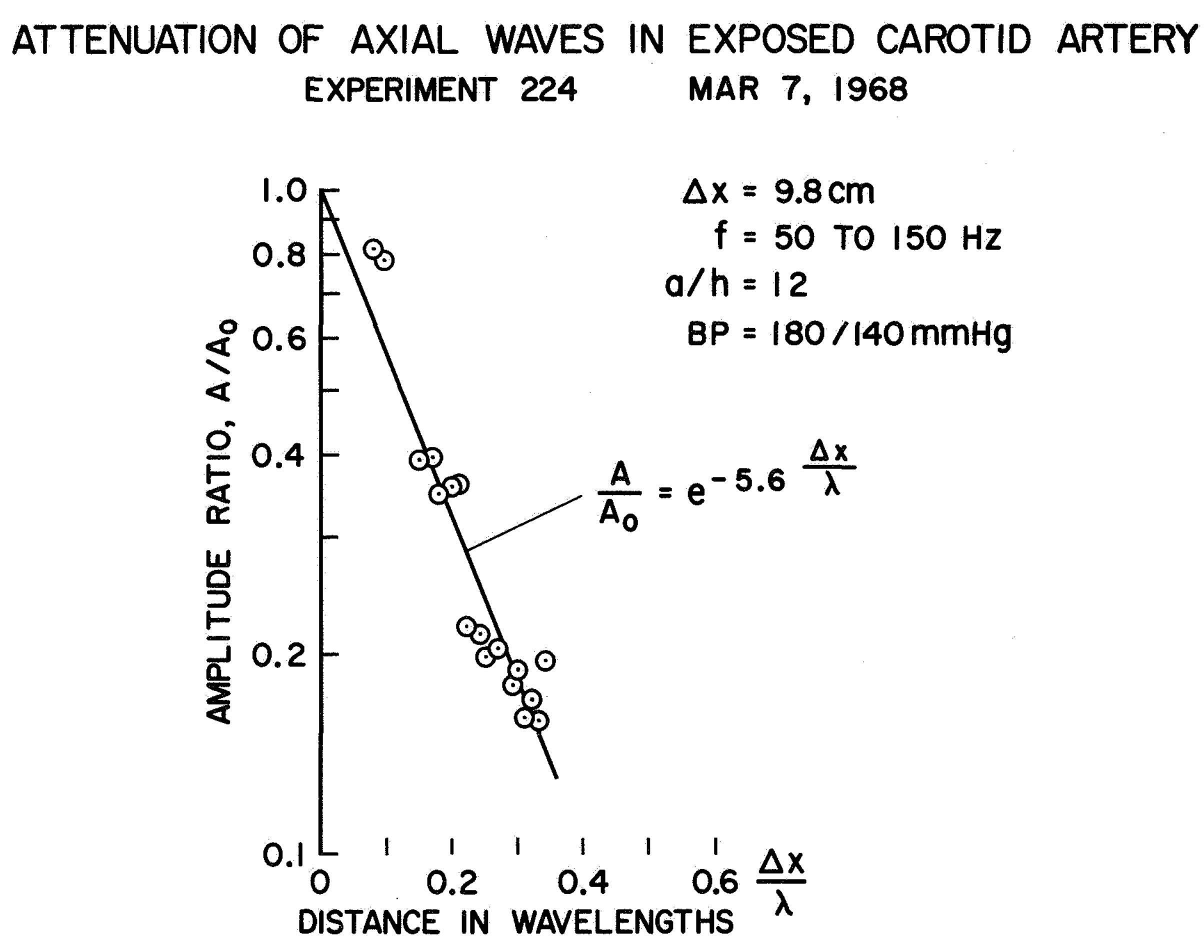

Figure 18. Representative attenuation pattern observed for axial waves in exposed carotid arteries. Each point corresponds to an average of at least three individual measurements. The data were obtained for a fixed target separation of 9.8 cm by varying the frequency and thus the distance travelled by the signals in terms of wave lengths.

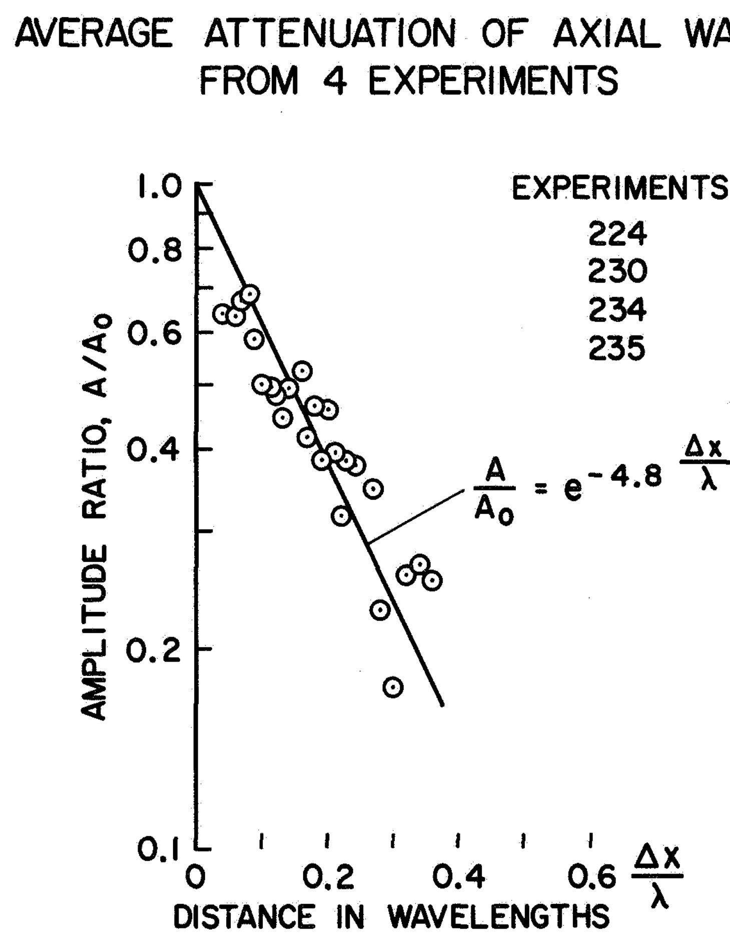

Figure 19. Average amplitude ratio from 4 dogs as a function of distance travelled in wave lengths.

TABLE I.

DATA ON RADIUS, WALL THICKNESS AND IN-VIVO STRETCH OF LEFT CAROTID ARTERIES IN DOGS

Experiment	Weight kg	2a (mm)	2h (mm)	a/h	x (cm)	x_o (cm)	$(x - x_o)/x_o$
198	26.4	4.0	.5	8.0	*	*	*
202	27.2	4.5	.7	6.4	6.8	5.5	.24
205	32.8	4.8	.7	6.8	*	*	*
210	29.5	5.0	.5	10.0	*	*	*
217	32.2	5.0	.5	10.0	10.0	6.5	.54
220	25.0	4.0	.5	8.0	*	*	*
224	28.6	4.0	.33	12.0	*	*	*
227	22.6	4.0	.33	12.0	8.5	6.5	.46
230	22.7	4.0	.5	8.0	8.4	6.1	.38
234	23.2	4.0	.5	8.0	*	*	*
235	28.6	5.0	.8	6.2	5.8	7.7	.33
236	35.4	5.0	.5	10.0	*	*	*

2a = outside diameter at normal blood pressure levels
h = wall thickness
x = in-vivo length
x_o = excised length

* indicates no measurement made

Average radius to wall thickness ratio (a/h) = 8.8
Average in-vivo stretch $[(x - x_o)/x_o]$ = .39